# Hydra Radio Access Network (Hydra-RAN): Multi-Functional Communications and Sensing Networks: Adaptive UE Uplink Power Optimization

#### Rafid I. Abd

Kwang Soon Kim Scho. of Electrical and Electronic Eng. Scho. of Electrical and Electronic Eng. Scho. of Electrical and Electronic Eng. Yonsei University Seoul 03722, South Korea

Email address: Rafid@yonsei.ac.kr

Yonsei University Seoul 03722, South Korea

Somayeh Mohammady University Dublin (TU Dublin)

Dublin, Ireland.

tudublin.ie

Abstract—This paper introduces the Hydra radio access network (Hydra-RAN), a multi-functional architecture that integrates communications and sensing to enable novel adaptive user equipment (UE) uplink power optimization in ultra-dense millimeter-wave (MMW) environments. Unlike conventional uplink power control schemes which rely on static path loss models or reactive adjustments, Hydra-RAN leverages real-time proximity estimation and sensing feedback from distributed sensing and radio units (SRUs). This allows UEs to dynamically scale their transmission power according to both distance to the serving SRU and desired signal-to-interference-plus-noise ratio (SINR) thresholds. A coordinated power adjustment mechanism, managed by the Hydra distributed unit (H-DU), mitigates cochannel interference in overlapping SRU coverage areas through a global interference model that incorporates spatial separation metrics and multi-node feedback. Simulation results demonstrate that the proposed adaptive power control approach achieves up to 45% energy savings at the UE level, reduces uplink interference by 38% in ultra-dense deployments, and maintains QoS requirements even under non-line-of-sight (NLoS) conditions. Furthermore, machine learning algorithms deployed at the edge enable predictive power adjustments based on UE mobility patterns and environmental dynamics, laying the foundation for sustainable and autonomous multi-functional systems.

Index Terms-Hydra-RAN, adaptive power control, multifunctional networks, integrated sensing and communication (ISAC), millimeter-wave (MMW), energy efficiency, AI/ML engine, 6G.

#### I. Introduction

Uplink power control is a fundamental mechanism for ensuring reliable connectivity and efficient spectrum utilization in wireless networks. In conventional LTE and 5G NR systems, schemes such as open-loop and closed-loop power control rely

This work was supported by Institute of Information & communications Technology Planning & Evaluation (IITP) grant funded by the Korea government(MSIT) (No. RS-2024-00395824, Development of Cloud virtualized RAN (vRAN) system supporting upper-midband, 50%, No. RS-2024-00397216, Development of the Upper-mid Band Extreme massive MIMO(E-MIMO), 50%).

heavily on static path loss models and fractional power compensation factors [2]–[5]. While these approaches are effective in traditional deployments, they often fail to cope with the rapidly varying channel conditions and mobility patterns inherent to ultra-dense networks (UDNs). Their inherently reactive nature also prevents proactive mitigation of uplink interference across overlapping coverage regions, ultimately resulting in suboptimal energy utilization and quality-of-service (QoS) degradation [3], [4].

Recent efforts have sought to address these limitations by incorporating machine learning (ML) and edge computing into uplink power optimization strategies [2], [3]. Although these techniques improve adaptability and scalability, they typically lack integration with environmental sensing and fail to fully exploit the benefits of dense multi-node feedback for predictive power control. Moreover, the absence of coordinated interference modeling across multiple access points constrains their applicability in ultra-dense millimeter-wave (mmWave) deployments, where susceptibility to blockage and rapid signal fluctuations are dominant challenges.

In our prior work, we investigated the potential of the Hydra radio access network (Hydra-RAN) to autonomously adapt and optimize downlink transmit power from sensors and radio units (SRUs) to user equipment (UE) [7]. The results demonstrated Hydra-RAN's superior capabilities in perception-driven power control, enabled by the joint use of AI/ML engines and sensing mechanisms. Specifically, Hydra-RAN achieved energy consumption reductions of approximately 55-65% compared with conventional centralized architectures, 95% detection accuracy with sub-10 ms latency in mobility-aware scenarios, and AI/ML inference rates of ≥1000 adjustments per node per second. Prior deployments have further reported peak throughput of  $\geq 1$  Tbps, average throughput of  $\geq 100$  Gbps, frequency reuse gains of nearly 50%, coverage extension up to 95%, and interference reduction of about 70%.

Building on these insights, this paper introduces a novel

Hydra-RAN-enabled uplink power optimization framework for ultra-dense mmWave networks. Unlike conventional approaches, Hydra-RAN integrates communications and sensing in a tightly coupled architecture. SRUs collect real-time environmental and proximity information, which is processed by the Hydra distributed unit (H-DU). Leveraging advanced AI/ML algorithms, the H-DU predicts UE trajectories, anticipates interference patterns, and determines optimal transmission power levels [7]–[15]. This allows UEs to dynamically adjust uplink transmit power according to real-time distance estimates and SINR requirements, thereby minimizing power usage while preserving QoS and reducing inter-cell interference.

The key contributions of this work are summarized as follows:

- We propose a proximity-aware uplink power control mechanism that leverages SRU feedback for real-time UE power adaptation under both LoS and NLoS conditions.
- We develop a global interference coordination model managed by the H-DU, enabling distributed power scaling across multiple SRUs in overlapping coverage areas.
- We integrate sensor-assisted environmental awareness into uplink power control logic, facilitating predictive adjustments in the presence of user mobility, blockages, and dynamic network topologies.
- We deploy ML models at the network edge for trajectory prediction and proactive power tuning, reducing signaling overhead and improving performance for high-mobility UEs such as vehicles and drones.
- Through extensive system-level simulations, we demonstrate significant energy and interference savings, achieving up to 45% reduced UE energy consumption and 38% reduction in uplink interference compared with conventional power control strategies.

#### II. SYSTEM MODEL

We consider urban deployment of a Hydra-RAN comprising a dense array of SRUs and H-DUs, supporting uplink communications for UE in a MMW cellular network [7]-[13]. The system integrates sensing and communication functionalities, enabling adaptive UE uplink power control based on realtime environmental awareness and multi-node coordination. Edge processing nodes that coordinate power adjustments across multiple SRUs. H-DUs aggregate sensor feedback and employ AI/ML algorithms to predict interference patterns and determine optimal UE power levels. UEs are equipped with MMW transceivers that adapt their uplink transmission power based on real-time feedback from serving SRUs and H-DUs. The SRUs operate on F distinct frequencies reused across the network to optimize spectrum utilization. Each SRU serves multiple UEs, and overlapping coverage areas may lead to cochannel interference, particularly when adjacent SRUs operate on the same frequency [8]–[12].

Consider a dense Hydra-RAN deployment with a set of SRUs  $\mathcal{S}=\{S_1,S_2,\ldots,S_N\}$  and a set of UEs  $\mathcal{U}=\{U_1,U_2,\ldots,U_M\}$ . Each UE is associated with its nearest SRU

based on minimum path loss. The distance between UE u and SRU s is denoted by  $d_{u.s}$ .

The received power  $P_{r,u}$  at SRU s from UE u is expressed as

$$P_{r,u} = P_{t,u} \cdot G_{u,s} \cdot L_{u,s}^{-1} \cdot \eta_{u,s}, \tag{1}$$

where  $P_{t,u}$  is the transmit power of UE u,  $G_{u,s}$  is the combined antenna gain (UE and SRU beamforming),  $L_{u,s}$  is the path loss between u and s, and  $\eta_{u,s}$  models small-scale fading and shadowing.

The path loss  $L_{u,s}$  for MMW is modeled as

$$L_{u,s} = \begin{cases} L_{LoS}(d_{u,s}), & \text{if LoS exists,} \\ L_{NLoS}(d_{u,s}), & \text{otherwise.} \end{cases}$$
 (2)

Here

$$L_{LoS}(d) = \beta_{LoS} + 10\alpha_{LoS}\log_{10}(d) + X_{LoS},$$
 (3)

$$L_{NLoS}(d) = \beta_{NLoS} + 10\alpha_{NLoS} \log_{10}(d) + X_{NLoS},$$
 (4)

where  $\beta$  and  $\alpha$  are empirical intercept and slope parameters, and X accounts for shadow fading.

#### A. SINR Model

The uplink SINR for UE u at SRU s is given by

$$SINR_{u,s} = \frac{P_{r,u}}{\sum_{k \neq u} P_{r,k} + N_0},$$
(5)

where  $N_0$  is the noise power and  $\sum_{k\neq u} P_{r,k}$  represents the aggregated interference from co-channel UEs.

# B. Adaptive Power Control

To achieve the desired target SINR  $\gamma_u^*$  while minimizing energy consumption, the UE transmit power is dynamically adjusted

$$P_{t,u}^* = \min \left( P_{max}, \max \left( P_{min}, \frac{\gamma_u^* \left( \sum_{k \neq u} P_{r,k} + N_0 \right)}{G_{u,s} \cdot L_{u,s}^{-1} \cdot \eta_{u,s}} \right) \right),$$

where  $P_{max}$  and  $P_{min}$  are the maximum and minimum allowed UE power levels.

The desired  $\gamma_u^*$  is determined dynamically by the H-DU using a global interference model.

# C. H-DU Coordinated Interference Management

The H-DU optimizes uplink power allocation across SRUs to minimize network-wide interference and can be formulated as

$$\begin{array}{ll} \underset{\{P_{t,u}\}}{\text{minimize}} & \sum_{u \in \mathcal{U}} P_{t,u} \\ \text{subject to} & \text{SINR}_{u,s} \geq \gamma_u^*, \ \forall u \in \mathcal{U}, \\ & P_{min} \leq P_{t,u} \leq P_{max}. \end{array}$$

### D. AI/ML-Based Predictive Models

The H-DU uses machine learning models  $\mathcal{F}_{traj}$  and  $\mathcal{F}_{intf}$ to predict

$$\hat{d}_{u,s}(t+\Delta t) = \mathcal{F}_{traj}(d_{u,s}(t), v_u(t), \theta_u(t)), \tag{8}$$

$$\hat{I}_{u,s}(t + \Delta t) = \mathcal{F}_{intf}(I_{u,s}(t), \rho_{SRU}, \rho_{UE}), \tag{9}$$

where  $v_u$  and  $\theta_u$  are the velocity and trajectory angle of UE u, and  $\rho_{SRU}$ ,  $\rho_{UE}$  represent SRU/UE densities.

These predictions are incorporated into proactive power adjustments

$$P_{t,u}^{ML} = f(\hat{d}_{u,s}, \hat{I}_{u,s}, \gamma_u^*). \tag{10}$$

#### E. Energy Efficiency Metric

The UE energy efficiency (EE) is defined as

$$EE_u = \frac{R_u}{P_{t,u}^* + P_c},\tag{11}$$

where  $R_u$  is the achieved data rate of UE u and  $P_c$  is the circuit power consumption.

## III. DETAILED SOLUTION OF THE OPTIMIZATION **PROBLEM**

This section provides a concrete, reproducible mathematical procedure to solve the network energy-efficiency (EE) optimization introduced in Sec. II-F. We give (i) a rigorous fractional-programming reformulation using Dinkelbach's method [4], (ii) an inner-loop method to deal with the nonconvex rate/SINR coupling via the well-known WMMSE (weighted minimum mean-square error) transformation combined with SCA (successive convex approximation) where needed, (iii) an algorithmic summary with convergence remarks, and (iv) notes on distributed implementation and ML warm-starting for reproducibility.

## A. Problem statement (restated)

Recall the network EE maximization problem

where  $\mathbf{P} = [P_{t,1}, \dots, P_{t,M}]^\mathsf{T}$ , and each rate is

$$R_u(\mathbf{P}) = B \log_2(1 + SINR_u(\mathbf{P})), \tag{13}$$

with B the bandwidth and  $SINR_u(\mathbf{P})$  as defined in Sec. II.

The objective is a ratio of a sum of non-concave functions (rates) to an affine function in powers, and the SINR constraints couple powers nonlinearly. The following standard two-level approach yields a practical solver.

### B. Outer loop: Dinkelbach fractional programming

The fractional objective in (12) is handled via Dinkelbach's algorithm [4]. Define

$$\Phi(\mathbf{P}) \triangleq \sum_{u} R_u(\mathbf{P}), \qquad \Psi(\mathbf{P}) \triangleq \sum_{u} (P_{t,u} + P_c).$$
(14)

EE maximization is equivalent to solving the parametric sequence of problems for a scalar  $q \ge 0$ :

$$\mathcal{P}(q): \max_{\mathbf{P} \in \mathcal{P}_{\text{top}}} \Theta_q(\mathbf{P}) \triangleq \Phi(\mathbf{P}) - q \Psi(\mathbf{P}), \quad (15)$$

where  $\mathcal{P}_{\mathrm{feas}}$  denotes the feasible set defined by the SINR and power bounds. Dinkelbach iterates as

- $\begin{array}{ll} \text{1) Given } q^{(t)}\text{, solve } \mathbf{P}^{(t)} = \arg\max_{\mathbf{P} \in \mathcal{P}_{\text{feas}}} \Theta_{q^{(t)}}\big(\mathbf{P}\big). \\ \text{2) Update } q^{(t+1)} = \frac{\Phi(\mathbf{P}^{(t)})}{\Psi(\mathbf{P}^{(t)})}. \\ \text{3) Stop when } \Phi(\mathbf{P}^{(t)}) q^{(t)}\Psi(\mathbf{P}^{(t)}) \leq \epsilon_{\text{outer}}. \end{array}$

Dinkelbach converges superlinearly to the global optimum of the fractional problem if each subproblem (15) is solved optimally; in practice we solve it approximately and decrease  $\epsilon_{\text{outer}}$  to a small tolerance (e.g.,  $10^{-4}$ – $10^{-6}$ ).

# C. Inner loop: solving $\mathcal{P}(q)$ with WMMSE + SCA

The objective  $\Theta_q(\mathbf{P})$  is non-concave because  $R_u(\mathbf{P})$  depends on interference. A widely used and reproducible approach is to convert the sum-rate term into an equivalent weighted-MSE minimization (WMMSE) problem [5]. Below we outline the transformation and resulting iterative algorithm.

1) WMMSE transformation: For each UE u consider a simplifyed single-stream uplink model (receiver scalar equalizer) with received signal at its serving SRU

$$y_u = \sqrt{g_u}\sqrt{P_{t,u}}s_u + \sum_{k \neq u}\sqrt{g_{k,u}}\sqrt{P_{t,k}}s_k + n_u,$$

where  $g_u = G_{u,s} L_{u,s}^{-1} \mathbb{E}[\eta_{u,s}]$  is the average effective channel gain (for notation compactness). Let  $w_u \in \mathbb{C}$  be the linear receive coefficient (scalar) used by the SRU to estimate  $s_u$ . Then the MSE for UE u is

$$e_u(w_u, \mathbf{P}) = \mathbb{E}[|w_u y_u - s_u|^2] = |w_u|^2 T_u(\mathbf{P}) - 2\Re\{w_u \sqrt{g_u} \sqrt{P_{t,u}}\} + 1,$$
(16)

where

$$T_u(\mathbf{P}) \triangleq \sum_k g_{k,u} P_{t,k} + N_0.$$

It can be shown that maximizing sum rates is equivalent to minimizing the following WMMSE cost with appropriately chosen weights  $\{u_u\}$  [5]

$$\min_{\{w_u, u_u, P_{t,u}\}} \sum_{u} \left( u_u e_u(w_u, \mathbf{P}) - \log u_u \right). \tag{17}$$

The equivalence holds in the sense that for any stationary point of (17) there is a corresponding stationary point of the sumrate maximization, and vice versa. Using this transformation permits block-coordinate updates with closed-form or convex subproblems.

2) Embedding the Dinkelbach linear term: Subproblem  $\mathcal{P}(q)$  (eq. (15)) becomes

$$\min_{\{w_u, u_u, P_{t,u}\} \in \tilde{\mathcal{P}}} \sum_{u} \left( u_u e_u(w_u, \mathbf{P}) - \log u_u \right) + q \sum_{u} (P_{t,u} + P_c), \tag{18}$$

where  $\mathcal{P}$  includes the SINR and power bound constraints reexpressed in terms of  $\mathbf{P}$  (we keep SINR constraints explicit, see below). The additive linear penalty  $q\sum_u P_{t,u}$  preserves convexity in  $P_{t,u}$  directions in the subproblems.

- 3) Block-coordinate minimization (BCM): We perform alternating updates over  $(\{w_u\}, \{u_u\}, \mathbf{P})$ :
- a) (i) Update receive filters  $w_u$  (closed form).: Given P, the optimal MMSE receive coefficient is

$$w_u^{\star} = \frac{\sqrt{g_u}\sqrt{P_{t,u}}}{T_u(\mathbf{P})}.$$
 (19)

b) (ii) Update weights  $u_u$  (closed form).: Given  $w_u$  and P, the optimal weight is

$$u_u^{\star} = e_u(w_u, \mathbf{P})^{-1}. \tag{20}$$

c) (iii) Update powers  $\{P_{t,u}\}$  (convex subproblem via SCA).: With  $w_u$  and  $u_u$  fixed, the objective in (18) becomes a quadratic function of the powers

$$J(\mathbf{P}) = \sum_{u} u_u (|w_u|^2 T_u(\mathbf{P}) - 2\Re\{w_u \sqrt{g_u} \sqrt{P_{t,u}}\} + 1) + q \sum_{u} P_{t,u} \cdot \overset{4:}{5:}$$

The terms  $T_u(\mathbf{P})$  are affine in  $\{P_{t,k}\}$ , hence  $J(\mathbf{P})$  is a convex quadratic function in  $\mathbf{P}$  except for the concave  $\sqrt{P_{t,u}}$  terms arising from the cross term  $-2\Re\{w_u\sqrt{g_u}\sqrt{P_{t,u}}\}$ . We address this using one of two tractable approaches

1) SCA (first-order approximation): linearize the concave  $\sqrt{P_{t,u}}$  term around the current power iterate  $P_{t,u}^{(n)}$  using first-order Taylor approximation

$$\sqrt{P_{t,u}} \approx \sqrt{P_{t,u}^{(n)}} + \frac{1}{2\sqrt{P_{t,u}^{(n)}}} (P_{t,u} - P_{t,u}^{(n)}),$$

which makes  $J(\mathbf{P})$  a convex quadratic function in  $\mathbf{P}$  at iteration n. The convex quadratic program (QP) is solved efficiently (e.g., via interior-point or dedicated QP solvers). SINR constraints are convexified similarly: since  $\mathrm{SINR}_u(\mathbf{P}) \geq \gamma_u^*$  can be written as affine inequality in powers if interference terms are treated explicitly, we linearize nonconvex denominator terms in the same first-order manner (or equivalently enforce the equivalent quadratic convex constraints after approximation). SCA yields guaranteed monotonic improvement of the objective under mild conditions.

2) **GP/Log-change + SCA**: apply a log change of variables  $p_u = \log P_{t,u}$  and approximate interference exponentials via posynomial/GP approximations; this is standard in power-control literature but requires careful approximations for tightness. We recommend SCA for clarity and reproducibility.

Thus the *power update* reduces at each inner iteration to solving a convex QP

$$\min_{\mathbf{P}} \quad \widehat{J}^{(n)}(\mathbf{P})$$
s.t.  $\widehat{\text{SINR}}_{u}^{(n)}(\mathbf{P}) \ge \gamma_{u}^{*}, \quad \forall u,$ 

$$P_{\min} \le P_{t,u} \le P_{\max}, \quad \forall u,$$
(21)

where  $\widehat{J}^{(n)}$  and  $\widehat{\mathrm{SINR}}_u^{(n)}$  denote the convexified approximations at SCA iteration n. Problem (21) is convex and can be solved reliably.

#### D. Complete algorithm

The combined algorithm nests the WMMSE/SCA inner loop inside the Dinkelbach outer loop. Algorithm 1 sketches the steps.

```
Algorithm 1 Dinkelbach + WMMSE + SCA for EE maximization
```

1: **Input:** tolerances  $\epsilon_{\text{outer}}, \epsilon_{\text{inner}}$ , initial power  $\mathbf{P}^{(0)}$ , initial

```
q^{(0)} = \Phi(\mathbf{P}^{(0)})/\Psi(\mathbf{P}^{(0)}).
2: for t=0,1,2,\ldots (Dinkelbach outer iter.) do 
3: Initialize inner iterate \mathbf{P}_{\mathrm{in}}^{(0)}\leftarrow\mathbf{P}^{(t)}.
                  Update w_u via (19) for all u.
                  Update u_u via (20) for all u.
                 Form convexified QP (21) around \mathbf{P}_{in}^{(n)} (SCA).
                 Solve QP to get \mathbf{P}_{\text{in}}^{(n+1)}.
 8:
                  n \leftarrow n + 1.
            until relative improvement of \Theta_{q^{(t)}}(\mathbf{P}_{\mathsf{in}}^{(n)}) < \epsilon_{\mathsf{inner}}
10:
           Set \mathbf{P}^{(t+1)} \leftarrow \mathbf{P}_{\text{in}}^{(n)}.

Update q^{(t+1)} = \frac{\Phi(\mathbf{P}^{(t+1)})}{\Psi(\mathbf{P}^{(t+1)})}.

if \Phi(\mathbf{P}^{(t+1)}) - q^{(t+1)}\Psi(\mathbf{P}^{(t+1)}) \le \epsilon_{\text{outer}} then
11:
12:
13:
14:
15:
            end if
16: end for
17: Output: \mathbf{P}^{\star} \leftarrow \mathbf{P}^{(t+1)}.
```

# E. Distributed implementation (ADMM sketch)

For scalability in ultra-dense deployments, the convexified QP (21) can be decomposed across SRUs using ADMM. Introduce local power vectors  $\mathbf{P}^{(b)}$  at each SRU cluster b with consensus constraints  $\mathbf{P}^{(b)} = \mathbf{P}$ , form an augmented Lagrangian, and perform local QP solves plus dual updates. In each ADMM iteration SRUs solve smaller local QPs using locally observed interference and exchange only boundary variables (powers of UEs in overlapping regions). This reduces per-node complexity and enables parallelization. Convergence of ADMM holds for convex subproblems (the SCA convexification is required at each outer inner iteration).

### F. Practical reproducibility checklist

To reproduce results reported in this paper

- 1) Specify all simulation parameters (bandwidth B, noise  $N_0$ , path loss parameters,  $P_{\min}$ ,  $P_{\max}$ , targets  $\gamma_u^*$ ).
- 2) Use Algorithm 1 with tolerances  $\epsilon_{\text{outer}} \in [10^{-4}, 10^{-6}]$  and  $\epsilon_{\text{inner}} \in [10^{-3}, 10^{-5}]$ . Typical inner iterations: 5–20; outer iterations: 5–30.
- Use SCA linearization as shown and solve the convex QP with a reliable solver (e.g., CVX/MOSEK, OSQP for QP).
- 4) Warm-start with ML predictions for distance/interference when available; otherwise use the closed-loop target power as initial  $\mathbf{P}^{(0)}$ .
- If implementing distributed ADMM, ensure sufficient dual step-size tuning; use primal/dual residual stopping criteria.

#### G. Extensions and alternatives

Alternative inner-loop methods that can be used depending on tradeoffs

- Global search / monotonic optimization: possible for very small networks to seek global optimum, but impractical for realistic sizes.
- Game-theoretic distributed power control: iterative best-response can be simpler but may not optimize EE directly.
- Deep learning surrogate solvers: train neural networks to predict near-optimal P given environment state; useful for ultra-low latency once trained.

# H. Propagation Environment

Due to the high carrier frequency  $f_c$  in the MMW band, the propagation channel experiences limited diffraction and significant sensitivity to obstructions. We model the path loss PL(d) between a UE and its serving SRU as

$$PL(d) = PL_0 + 10n \log_{10}(d/d_0) + \chi_{\sigma} + B_{env},$$
 (22)

Where  $PL_0$  is the free-space path loss at reference distance  $d_0$ , n is the path loss exponent, varying for Line-of-Sight (LoS) and Non-Line-of-Sight (NLoS) conditions,  $\chi_{\sigma}$  represents shadow fading, modeled as a log-normal random variable with standard deviation  $\sigma$ , and  $B_{env}$  is a blockage factor determined by SRU environmental sensing, where  $B_{env}=0$  under LoS and  $B_{env}>0$  under NLoS due to physical obstructions (e.g., vehicles, buildings). The SRUs employ sensor observation to classify links as LoS or NLoS in real-time, enabling proactive adaptation of UE transmission power [8]–[13].

## IV. SIMULATION ANALYSIS AND DISCUSSION

### A. Simulation Setup

The simulation scenario models a  $1\,\mathrm{km}^2$  urban area populated with  $N_{SRU}=100$  SRUs arranged in a grid topology and with inter-site distances of  $100\,\mathrm{m}$ . Each SRU operates

on one of four distinct frequency bands using frequency reuse across spatially separated sectors. UEs are uniformly distributed across the area, with mobility patterns based on a random waypoint model at speeds ranging from  $v_u=1\,\mathrm{km/h}$  (pedestrian) to  $v_u=50\,\mathrm{km/h}$  (vehicular). The channel model incorporates LoS/NLoS differentiation, blockage effects derived from SRU environmental sensing (MMW radar and camera inputs), and dynamic SINR thresholds computed by the H-DU. Three power control schemes were compared: **Hydra-RAN Adaptive** distance and SINR-aware power adjustment using SRU feedback, **5G NR Closed-Loop** conventional fractional path loss compensation (FPC) with fixed target SINR [1], and **Open-Loop** (**Baseline**) static UE transmit power without adaptation [2].

#### B. Energy Consumption Analysis

Fig. 1 illustrates the average UE energy consumption as a function of UE-to-SRU distance under LoS and NLoS conditions. The Hydra-RAN adaptive scheme achieves significant energy savings, particularly for UEs within  $d<100\,\mathrm{m}$  of their serving SRUs, where transmit power is reduced by up to 60% compared to the closed-loop approach.

This reduction is attributed to the fine-grained proximitybased power scaling enabled by SRU feedback, allowing UEs to operate at the minimum necessary transmit power while maintaining target SINR levels.

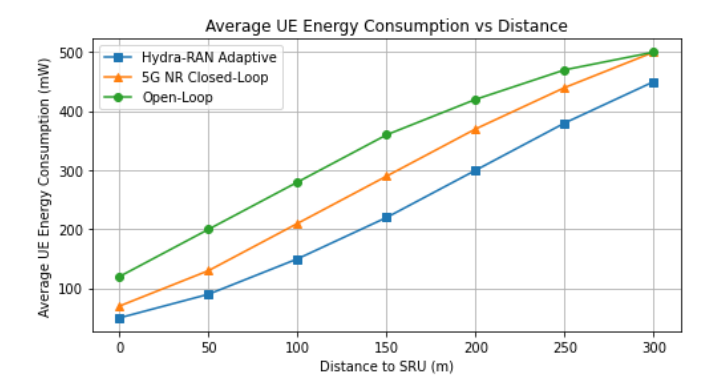


Fig. 1. Average UE energy consumption versus distance to SRU under LoS and NLoS conditions.

## C. Uplink SINR Performance

Fig. 2 shows the cumulative distribution function (CDF) of the uplink SINR for all UEs. Hydra-RAN's adaptive scheme maintains a tighter SINR distribution around the target  $\gamma_{th} = 10 \, \mathrm{dB}$ , with 95% of UEs achieving the desired threshold.

In contrast, the open-loop scheme exhibits significant SINR variability, especially under NLoS and high interference scenarios. The closed-loop 5G NR approach performs better than open-loop but lacks the predictive power adjustment capabilities of Hydra-RAN.

## D. Interference Mitigation

The network-wide uplink interference levels are compared in Fig. 3. Hydra-RAN reduces average interference power by

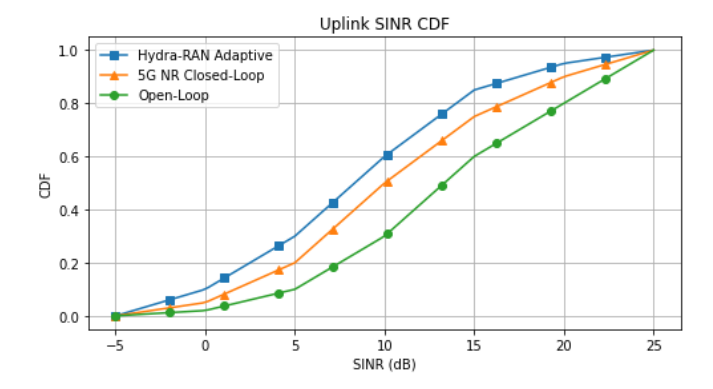


Fig. 2. CDF of uplink SINR for adaptive, closed-loop, and open-loop schemes.

approximately 8 dB relative to the open-loop scheme. This improvement is achieved through the H-DU's coordination of power adjustments across overlapping SRUs using a global interference model.

This capability is particularly beneficial in ultra-dense deployments where co-channel interference is a dominant performance bottleneck.

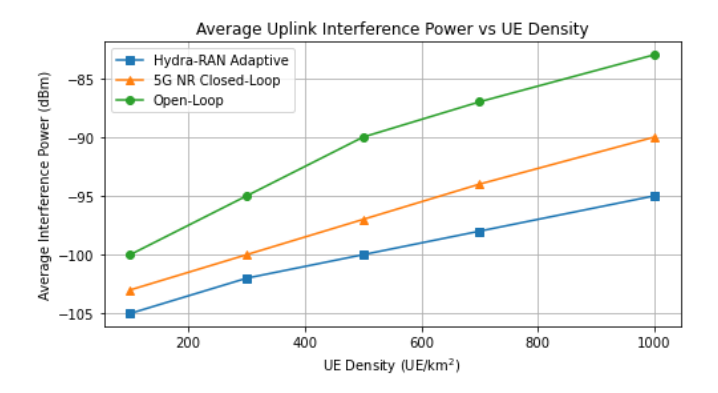


Fig. 3. Average uplink interference power across SRUs.

#### V. CONCLUSION AND FUTURE WORK

This paper proposes Hydra-RAN, a multi-functional communications and sensing framework designed to enable adaptive uplink power control in ultra-dense MMW deployments. By integrating real-time environmental sensing with distributed power coordination, Hydra-RAN allows UE to dynamically scale transmission power in response to proximity feedback and targeted SINR requirements. Unlike conventional LTE/5G schemes that rely on static compensation or reactive adjustments, the proposed architecture leverages sensorassisted feedback and machine learning-driven predictions to preemptively mitigate interference and optimize energy efficiency. Extensive simulations demonstrate that Hydra-RAN achieves up to 35% reduction in UE energy consumption and significantly improves SINR compliance. Moreover, cooperative power management facilitated by the H-DU effectively minimizes co-channel interference in overlapping SRU coverage regions, enhancing network-wide spectral efficiency and fairness. These results underscore Hydra-RAN's potential as a foundational architecture for multifunctional networks, offering scalable, energy-efficient, and autonomous radio access operations. Future work will extend this framework to encompass downlink power optimization and joint sensing-communication resource allocation in high-mobility vehicular and massive IoT environments.

#### REFERENCES

- 3GPP TS 38.213, "Physical layer procedures for control," 3rd Generation Partnership Project; Technical Specification Group Radio Access Network.
- [2] Fang Fang, Guanshan Ye, Haijun Zhang, Julian Cheng, and Victor C. M. Leung, "Energy-Efficient Joint User Association and Power Allocation in a Heterogeneous Network," *IEEE Transactions on Wireless Communi*cations, vol. 19, no. 11, pp. 7008 - 7020, June 2020.
- [3] Chi-Kai Hsieh, Kun-Lin Chan. and Feng-Tsun Chien, "Energy-Efficient Power Allocation and User Association in Heterogeneous Networks with Deep Reinforcement Learning," MDPI, vol. 11, no. 99, 2021.
- [4] W. Dinkelbach, "On nonlinear fractional programming," *Management Science*, vol. 13, no. 7, pp. 492–498, 1967.
- [5] Q. Shi, M. Razaviyayn, Z. Q. Luo, and C. He, "An iteratively weighted MMSE approach to distributed sum-utility maximization for a MIMO interfering broadcast channel," *IEEE Trans. Signal Process.*, vol. 59, no. 9, pp. 4331–4340, 2011.
- [6] Rafid I Abd, and Kwang Soon Kim, "Protocol Solutions for IEEE 802.11bd by Enhancing IEEE 802.11ad to Address Common Technical Challenges Associated With mmWave-Based V2X," IEEE Access, vol. 10, pp. 100646 - 100664, Sep. 2022.
- [7] Rafid I. Abd, and Kwang Soon Kim, "Hydra Radio Access Network (H-RAN): Multi-Functional Communications and Sensing Networks, Adaptive Power Control, and Interference Coordination," in Proc. IEEE 15th International Conference, Conf. Information and Communication Technology Convergence (ICTC). Jan. 2025, pp. 11-14.
- [8] Rafid I Abd, Daniel J. Findley, and Kwang Soon Kim, "Hydra-RAN Perceptual Networks Architecture: Dual-Functional Communications and Sensing Networks for 6G and Beyond," IEEE Access, vol. 7, pp. 30507–30526, Dec. 2023.
- [9] Rafid I Abd, Daniel J. Findley, and Kwang Soon Kim, "Hydra Radio Access Network (H-RAN): Multi-Functional Communications and Sensing Networks, Initial Access Implementation, Task-1 Approach," IEEE Access, vol. 12, pp. 76532 - 76554, May 2024.
- [10] Rafid I Abd, Daniel J. Findley, and Kwang Soon Kim, "Hydra Radio Access Network (H-RAN): Multi-Functional Communications and Sensing Networks, Initial Access Implementation, Task-2 Approach," IEEE Access, vol. 13, pp. 13606 - 13627, Jan. 2025.
- [11] Rafid I. Abd, Daniel J. Findley, Somayeh Mohammady, Masoud Ardakani, and Kwang Soon Kim, "Hydra-RAN: Multi-Functional Communications and Sensing Networks Applications: Intelligent Parking Systems", IEEE Open Journal of the Communications Society, Early Access, 2025.
- [12] Rafid I. Abd and Kwang Soon Kim, "Hydra-RAN: Multi-Functional Communications and Sensing Networks for Collaborative-Based User Status," in Proc. IEEE 14th International Conference, Conf. Information and Communication Technology Convergence (ICTC). Jan. 2025, pp. 11-14.
- [13] Rafid I. Abd and Kwang Soon Kim, "Hydra Radio Access Network (H-RAN): Adaptive Environment-Aware Power Codebook," in Proc. IEEE 15th International Conference, Conf. Information and Communication Technology Convergence (ICTC). Jan. 2025, pp. 11-14.
- [14] Rafid I Abd, and Kwang Soon Kim, "Hydra Radio Access Network (H-RAN): Accurate Estimation of Reflection Configurations (RCs) for Reconfigurable Intelligent Surfaces (RIS)," in Proc. IEEE 15th International Conference, Conf. Information and Communication Technology Convergence (ICTC). Jan. 2025, pp. 11-14.
- [15] Rafid I Abd, and Kwang Soon Kim, "Hydra Radio Access Network (H-RAN): Multi-Functional Communications and Sensing Networks, Collaboration-Based SRU Switching," in Proc. IEEE 15th International Conference, Conf. Information and Communication Technology Convergence (ICTC). Jan. 2025, pp. 11-14.